Assessing the Structure of Octastate Molecular Switches Using 1H NMR Density Functional Theory Calculations

Hadj Mohamed, Slim; Quertinmont, Jean; Delbaere, Stéphanie; Sanguinet, Lionel; Champagne, Benoît

Published in:
The Journal of Physical Chemistry C

DOI:
10.1021/acs.jpcc.7b11221

Publication date:
2018

Document Version
Publisher's PDF, also known as Version of record

THE JOURNAL OF PHYSICAL CHEMISTRY C

Article

Cite This: J. Phys. Chem. C 2018, 122, 1800−1808

pubs.acs.org/JPCC

Assessing the Structure of Octastate Molecular Switches Using ^{1}H NMR Density Functional Theory Calculations

Slim Hadj Mohamed,[†,‡,⊥] Jean Quertinmont,[‡,⊥] Stéphanie Delbaere,[§] Lionel Sanguinet,*[,∥] and Benoît Champagne*[,‡]

[†]Laboratory of Natural Substances, Faculty of Sciences, University of Sfax, 3038 Sfax, Tunisia

[‡]Laboratory of Theoretical Chemistry, Theoretical and Structural Physical Chemistry Unit, Namur Institute of Structured Matter, University of Namur, rue de Bruxelles, 61, B-5000 Namur, Belgium

[§]LASIR, Université de Lille, CNRS UMR 8516, F-59000 Lille, France

[∥]MOLTECH-Anjou, Université d'Angers, CNRS-UMR 6200, F-49045 Angers, France

ABSTRACT: Density functional theory calculations are used to reveal the relationships between the structures, energies, and NMR signatures of an octastate molecular switch composed of a dithienylethene (DTE) unit covalently linked to an indolino[2,1-*b*]oxazolidine (BOX) moiety through an ethylenic junction. Both the DTE and BOX moieties can adopt open or closed forms. The ethylenic junction can be *Z* or *E*, but the latter has been confirmed to be, by far, more stable than the former for all BOX/DTE combinations. In addition, when the DTE is open, the two thienyl units can fold to form parallel conformers, by opposition to the antiparallel or unfolded conformers. Usually parallel conformers present a higher energy than the antiparallel ones, but in the case of compound **2** having a bulky substituent (R = *p*Ph-SMe) on the terminal thienyl group, the enthalpy of one conformer is very close (1−2 kJ mol^{-1}) to that of the most stable antiparallel one, making photocyclization less efficient. These conformational differences and the presence of parallel DTE forms have been substantiated by analyzing experimental ^{1}H NMR chemical shifts in light of their calculated values. These ^{1}H NMR chemical shift calculations led to the following statements: (i) Going from state I (DTE open, BOX closed) to state II (both DTE and BOX are open) the H_8 proton of compound **1** (R = Me) is deshielded by ∼0.15 ppm. (ii) The deshielding of H_8 proton of compound **2** is larger and attains 0.41 ppm whereas H_7 is more shielded by 0.11 ppm. (iii) Then, going from compound **1** to compound **2** leads to deshielding of both H_7 and H_8 protons. As a consequence, the difference of photochromism gating efficiency among compounds **1**, **2**, and **3** (R = *p*Ph-OMe) can be attributed to the stabilization of parallel conformer due to an establishment of an intramolecular interaction with BOX opening.

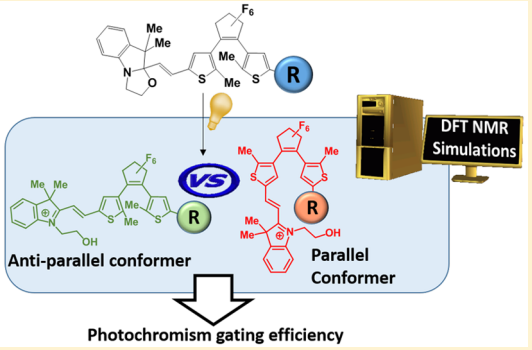

I. INTRODUCTION

The combination at a molecular level of several switchable units in order to elaborate multiresponsive molecular systems continues to raise a strong interest due to their promising application in many fields such as logic gates or high-density optical memories to name a few.[1,2] Indeed, the combination of *n* two-state switches shapes a multiswitch system that can exhibit up to 2^n various metastable states. Numerous molecular systems combining different types of switch moieties have been reported[3−6] with a particular interest for photo- and redox-active materials.[7−9] In this context, numerous systems incorporating a diarylethene (DAE) unit, undoubtedly the most studied photoswitch family,[10−20] associated with a redox probe, with a photochromic unit and even with a pH-sensitive moiety were reported.[21−23] However, this association could lead to a strong modification of the switching abilities of the DAE moiety and lead in the most interesting cases to a complete control of the photochromism behavior on demand. Indeed, the material addressability and nondestructive readout capacity by light are the major challenges to overcome in the design of efficient memory devices at the molecular scale. Concerning the DAE based systems, the control of the photochromism is generally obtained either by a strong modification of the electronic properties of the molecular system or due to geometric considerations. Concerning these last ones, it should be mentioned that systems based on the DAE unit can exist in both parallel and antiparallel conformations. Parallel conformers have the methyl group of both thiophenes pointing toward the same direction while they point in opposite directions for the antiparallel ones, and only the latter can photocyclize according to the Woodward−Hoffmann rules.

In this context, the elaboration of a biphotochrome molecular switch composed of a dithienylethene (DTE) unit

Received: November 13, 2017
Revised: December 19, 2017
Published: December 20, 2017

DOI: 10.1021/acs.jpcc.7b11221
J. Phys. Chem. C 2018, 122, 1800−1808

Scheme 1. Schematic Representation of the Eight Possible Metastable States of BOX−DTE Hybrids Resulting from the Combination of the Open/Closed (O/C) Form of the BOX (□/■) and DTE (○/●) Units Linked Together by an Ethylenic Bridge in a *trans*/*cis* (T/C, △/▲) Configuration

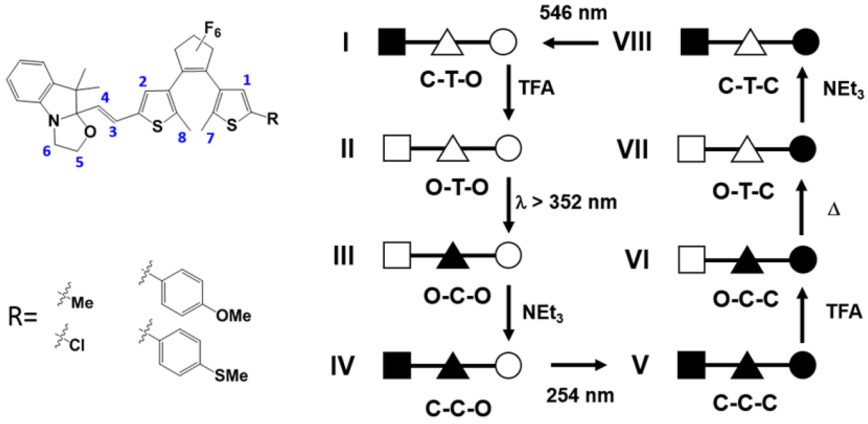

covalently linked to an indolino[2,1-*b*]oxazolidine (BOX) moiety through an ethylenic junction has demonstrated complementary features (Scheme 1). Besides, the results from the 8 (2^3) reachable states, thanks to the open and closed forms of both DTE and BOX units and the *Z*/*E* isomerization of the ethylenic junction, have demonstrated that the photochromism of the DTE core is largely influenced by the status of the BOX unit.[24] In fact, the photocyclization of the DTE is largely diminished when the oxazolidine ring is open (from state II to VII). More important, the efficiency of this photochemical process quenching is largely influenced by the nature of the second substituent borne by the DTE core. In fact, phenyl groups substituted by a donating group [R = *p*Ph-SMe (**2**), *p*Ph-OMe (**3**)] increase the photocyclization quenching (less than 1% of cyclized form is observed) in comparison to the more classical DTE substituent (R = Cl or Me (**1**) with, respectively, 4% and 10%).

To the best of our knowledge, the influence of the BOX opening on the reduction of the DTE photocyclization capacity was already apprehended using theoretical tools such as time-dependent density functional theory (TDDFT) but without geometrical consideration.[25] To fill this gap, the conformer distribution between parallel and antiparallel ones has to be determined for all different states of the different DTE/BOX hybrids. For such a purpose, the differences in the chemical shift of proton NMR (especially those of the methyl groups) can generally be used, but this requires NMR chemical shift calculations for both conformers.[26] In this context, *ab initio* NMR chemical shift calculations constitute a useful tool for interpreting and assigning NMR spectra of complex molecules.[27−29] The development of accurate *ab initio* methods including electron correlation, solvent, ro-vibrational, relativistic, and temperature effects has led to predict quantitatively the nuclear magnetic shielding tensors. In parallel, density functional theory (DFT) methods with *ad hoc* exchange-correlation functionals, which can be employed to systems containing hundreds of atoms and more,[30] are very accurate, or at least, their errors are systematic and can easily be corrected, for instance, by using linear scaling procedures,[31−36] opening the way to applications to a broad range of compounds of increasing complexity. In addition, errors with respect to high-level *ab initio* methods are generally small and less than 0.2 ppm for ^{1}H.[33,35] These first-principles NMR investigations have contributed to determination of the structures as well as the conformations and configurations of complex systems, including supramolecular host−guest compounds,[37] elatenyne,[38] strychnine,[39] heparin trisaccharide,[40] *Z*/*E* isomers of alkyl phenyl ketone phenylhydrazones,[41] and poly(vinyl chloride) oligomers bearing unsaturated and branched defects.[42] They have also played a key role in the assignment or reassignment of the stereostructure of organic and natural products.[43−45] On the other hand, to our knowledge, such a combined theoretical−experimental approach was not yet applied to molecular switches.

Concerning the studied BOX/DTE hybrids, the opening/closure of the oxazolidine ring induces a strong modification of the ^{1}H NMR spectrum facilitating the complete identification and quantification of the generated species.[24] The strong variation of the acceptor ability of BOX during its opening leads to an important deshielding of the different nuclei chemical shifts hiding a potential effect of conformational change on it. As a consequence, the increase of the chemical shifts of methyl protons (nuclei 7, Scheme 1) of the thienyl group bearing the R substituent with the BOX opening is until now the only element suggesting a variation of the parallel and antiparallel conformer ratio. Unfortunately, with the latter being strongly correlated to the nature of substituent R, the simple analysis of the NMR spectrum is not accurate enough to determine the influence of R on the parallel and antiparallel conformer ratio, and, then, on the photochromism gating.

In order to fill this gap, we have carried out a comparative theoretical study on different BOX/DTE hybrids where the second substituent borne by the DTE is, respectively, a Me (**1**), (Cl), and *p*Ph-SMe (**2**), *p*Ph-OMe (**3**) group. After their comparison to experimental results, our objective is to determine, using DFT, in the same time the electronic and conformational influence of the BOX status on the DTE photocyclization process. This paper is organized as follows. The next section summarizes the key computational aspects. Section III presents and discusses the results before conclusions are drawn in Section IV.

II. COMPUTATIONAL METHODS

The geometries of the 8 states were optimized using DFT with the M06[46] XC functional and the 6-311G(d) basis set. The M06 XC functional was selected owing to its overall good performance for estimating geometrical parameters and thermodynamics. For each state, the potential energy surface

DOI: 10.1021/acs.jpcc.7b11221
J. Phys. Chem. C 2018, 122, 1800−1808

Table 1. M06/6-311G(d) Relative Enthalpies ($\Delta H°$) and Gibbs Free Energies ($\Delta G°$) for the Most Stable Conformers of the 8 States of Compound 1[a]

state	$\Delta G°$ [kJ mol^{-1}]	$\Delta\Delta G°$ [kJ mol^{-1}]	% (*cis*)	$\Delta H°$ [kJ mol^{-1}]	$\Delta\Delta H°$ [kJ mol^{-1}]	% (*cis*)
c-c-o	15.9	−15.9	0.17%	12.3	−12.3	0.69%
c-t-o	0.0			0.0		
c-c-c	52.1	−16.3	0.14%	43.0	−14.9	0.25%
c-t-c	35.9			28.1		
o-c-c	210.3	−25.4	0.004%	205.7	−18.9	0.05%
o-t-c	184.9			186.8		
o-c-o	170.6	−23.8	0.007%	167.3	−7.9	3.94%
o-t-o	146.8			159.4		

[a]Differences of enthalpies [$\Delta\Delta H° = \Delta H°(trans) - \Delta H°(cis)$] and Gibbs free energies ($\Delta\Delta G°$) for each pair of *cis*−*trans* isomers are also provided together with the corresponding *cis* population calculated using the Maxwell−Boltzmann distribution. Solvent effects were taken into account using the IEFPCM scheme (solvent = acetonitrile).

Table 2. IEFPCM (Solvent = Acetonitrile)/M06/6-311G(d) Relative Enthalpies ($\Delta H°$, kJ mol^{-1}) and Representative Geometrical Parameters (φ_1 and φ_1 in deg and R_{CC} in Å) of the 8 Most Stable Conformers of States I and II of Compounds 1 and 2

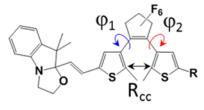

State **I**

	R = Me				R = PhSMe			
	φ_1	φ_2	R_{CC}	ΔH^0	φ_1	φ_2	R_{CC}	ΔH^0
Conformer a	-38.4	-53.8	3.512	0.6	-38.5	-53.6	3.526	0.3
Conformer b	54.5	38.0	3.522	0.0	54.7	39.3	3.518	0.2
Conformer c	54.0	38.0	3.518	0.1	54.4	39.2	3.520	0.0
Conformer d	-38.4	-53.8	3.513	0.2	-39.0	-53.8	3.525	0.6
Conformer e	-40.5	115.8	4.129	9.3	-44.3	120.7	4.119	8.3
Conformer f	54.6	-140.6	4.258	6.6	70.2	-143.5	4.165	1.8
Conformer g	54.3	-140.5	4.255	6.7	60.3	-143.8	4.236	4.2
Conformer h	-40.2	115.8	4.129	9.0	-115.0	40.7	4.121	8.5

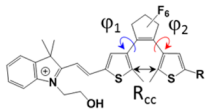

State **II**

	R = Me				R = PhSMe			
	φ_1	φ_2	R_{CC}	ΔH^0	φ_1	φ_2	R_{CC}	ΔH^0
Conformer a	55.1	39.1	3.533	0.0	57.2	39.8	3.544	0.0
Conformer b	-39.3	-54.2	3.529	1.3	-40.3	-55.8	3.528	1.4
Conformer c	55.7	38.7	3.542	5.5	55.7	40.1	3.532	5.8
Conformer d	-40.1	-54.7	3.532	6.5	-40.5	-55.2	3.533	6.6
Conformer e	138.8	-55.3	4.241	7.3	137.3	-54.5	4.237	7.3
Conformer f	-42.1	116.6	4.133	9.1	-42.3	116.6	4.130	9.2
Conformer g	139.9	-56.9	4.232	11.8	143.7	-68.8	4.184	1.3
Conformer h	-42.1	116.8	4.136	14.9	-41.7	116.0	4.126	14.8

has been probed in a systematic way, i.e., by varying stepwise the torsion angles around the CC single bonds, in order to locate the minima, characterized by real vibrational frequencies. Only the conformers within a 12 kJ mol^{-1} range from the most stable one are considered further (at T = 298.15 K, if their energies differ by 12 kJ mol^{-1} the corresponding populations are in the 99:1 ratio). Their standard enthalpy ($H°$), entropy ($S°$), and Gibbs enthalpy ($G°$) were then evaluated for T = 298.15 K and P = 1 atm. A scaling factor of 0.97 was used for all vibrational frequencies. Then, the isotropic shielding constants were evaluated using the B3LYP XC functional and the 6-311+G(2d,p) basis set in combination with the GIAO method.[47] This approach was already employed and its performance substantiated in ref 48. Then, the chemical shifts

DOI: 10.1021/acs.jpcc.7b11221
J. Phys. Chem. C 2018, 122, 1800−1808

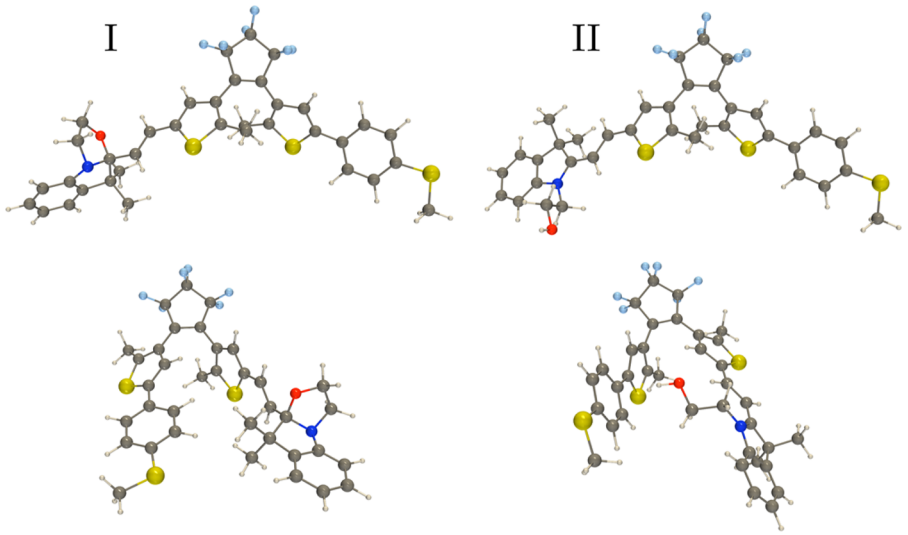

Figure 1. Sketch of representative folded (parallel, bottom) and unfolded (antiparallel, top) conformers of **2** (I) and **2** (II) as determined from M06/6-311G(d) geometry optimization using the IEFPCM scheme (solvent = acetonitrile).

were evaluated as $\delta = \sigma_{ref} - \sigma$, where σ_{ref} is the shielding constant of ^{1}H of tetramethylsilane (TMS) as reference compound. On the basis of the Gibbs enthalpies, Maxwell–Boltzmann averaging of the chemical shifts was carried out for the conformers within the 12 kJ mol^{-1} range. Solvent (acetonitrile) effects were taken into account by using the IEFPCM approach[49] for the geometry optimizations, the evaluation of the thermodynamic state functions, and the calculations of the isotropic shielding constants of all compounds and states. All calculations were performed using the Gaussian 09 program package.[50] An ultrafine integration grid has been employed for all calculations.

III. RESULTS AND DISCUSSION

III.A. Geometrical Optimization of the Different Metastable States. As mentioned above, the BOX–DTE hybrids are known to exhibit eight different metastable states depending on the status of the three different switchable units. However, the existence of an equilibrium between several conformers as long as the DTE unit is in its open form should be considered to rationalize the photochromic behavior of these compounds. This leads to a potentially large number of conformers. In order to select the most stable ones, for compound **1**, we have first compared the *cis* and *trans* isomers by performing geometry optimizations. At this stage, the enthalpies and Gibbs free energies were calculated only for the most stable conformer of each state. They are reported in Table 1 together with the *cis*–*trans* relative values and the *cis* population, as computed with the Maxwell–Boltzmann distribution. In agreement with experimental results from Szaloki et al.,[51] the *trans* isomers are more stable than the *cis* ones. The populations of the latter range from 0.004% to 0.17% according to the Gibbs free energies and from 0.05% to 4% when using the enthalpies. From now on, we only consider the *trans* isomers.

In order to confirm the mechanism responsible for the gated DTE photocyclization of these biphotochromes, the optimized structures of the I and II states of compounds **1** and **2** were analyzed in detail, and their enthalpies are compared in Table 2 with representative geometrical parameters. For each compound and state, eight low-energy conformers, labeled from a to h, were obtained on the basis of the 12 kJ mol^{-1} range. The two dihedral angles between the hexafluorocyclopentene ring and the thiophenes, φ_1 and φ_2, schematically shown in Table 2, allow distinguishing between four antiparallel conformers, where φ_1 and φ_2 are of the same sign and both vary between 35° and 55° (conformers a–d), and four parallel conformers where φ_1 and φ_2 have opposite signs and vary between 40–70° and 115–145° (conformers e–h). The distance (R_{CC}) between the thiophene carbons involved in the photocyclization also allows this distinction because for antiparallel conformers R_{CC} ∼ 3.5 Å while for the parallel ones, R_{CC} is larger than 4.1 Å.

In the case of compound **1** (R = Me), the most stable conformers are unfolded/antiparallel, irrespective of the open (I)/closed (II) state of the BOX. Indeed, the difference of enthalpy between the most stable parallel and antiparallel conformers is 6.6 and 7.3 kJ mol^{-1} for state I and state II, respectively. The situation is different for compound **2** (R = *p*Ph-SMe). When BOX is closed, the most stable folded conformer (Figure 1) presents an enthalpy similar ($\Delta H° \leq 1.8$ kJ mol^{-1}) to those of the four unfolded conformers. Then, when BOX is open, the second most stable conformer ($\Delta H°$ = 1.3 kJ mol^{-1}) is folded, owing to stabilizing intramolecular interactions between the aromatic substituent and the hydroxyl function (Figure 1). Additional calculations on compound **3** (R = *p*Ph-OMe, not reported here) highlight similar effects associated with stabilizing intramolecular interactions. In a subsequent step, the relative populations of the folded and unfolded conformers were calculated using the electronic energy as well as the enthalpy, and the Gibbs enthalpy (Table 3).

The percentages of folded conformers evaluated from the electronic energy and the enthalpy are in agreement, highlighting the increased stability of the folded conformers in compound **2** with respect to **1**. On the other hand, when including entropy contributions these effects are strongly damped and the percentage of folded conformers goes down to 4% for the o-t-o form of compound **2**. This originates from the decrease of entropy of the folded conformers because the intramolecular interactions reduce the flexibility of the molecule. Still, we consider that these entropy effects are probably slightly overestimated because the IEFPCM calcu-

DOI: 10.1021/acs.jpcc.7b11221
J. Phys. Chem. C 2018, 122, 1800–1808

Table 3. Percentage of Folded/Unfolded Conformers for Compounds 1 and 2 in Their c-t-o (I) and o-t-o (II) States As Determined from Different Thermodynamic State Functions Evaluated at the M06/6-311G(d) Level Using the IEFPCM Scheme (Solvent = Acetonitrile) and a Scaling Factor of 0.97 for the Vibrational Frequencies

	electronic energy	$H°$	$G°$
	Compound **1**, R = Me		
(I) c-t-o	5.0/95.0	4.8/95.2	11.0/89.0
(II) o-t-o	4.9/95.1	4.8/95.2	7.7/92.3
	Compound **2**, R = *p*Ph-SMe		
(I) c-t-o	20.6/79.4	17.2/82.8	5.0/95.0
(II) o-t-o	30.5/69.5	27.8/72.2	4.1/96.9

lations do not account for the solvent molecules reorganization upon folding/unfolding.

III.B. ^{1}H NMR Chemical Shifts of Biphotochrome 1 in Its Eight States. Subsequently, the ^{1}H NMR chemical shifts of molecule **1** for each of its eight states were calculated at the B3LYP/6-311+G(2d,p)//M06/6-311G(d) level. The averaged ^{1}H NMR chemical shifts are reported in Table 4 together with the experimental values from ref 51. When DTE is open, these averages were performed over the antiparallel conformers only. According to their position and spectral range, they are discussed in four different groups: aromatic (1 and 2), vinylic (3 and 4), aliphatic (5 and 6), and methyl (7 and 8). In a first step, the reliability of the computational procedure is confirmed by only considering the states where the DTE is closed. Indeed, Woodward−Hoffmann rules apply to only one conformer, contrary to the states where DTE is open where both parallel or antiparallel (*vide infra*) conformers have to be considered.

DFT calculations reproduce, for all states, the δ ordering of protons H_1 and H_2; i.e., H_2 is logically more deshielded than H_1 [due to the positive mesomeric effect of the methyl substituent], and this phenomenon is exalted when the BOX is open. The average calculated difference $[\delta(H_2) - \delta(H_1)]$ amounts to 0.39 ppm for all states with the closed BOX, which is in good agreement with the experimental average value of 0.33 ppm. The BOX opening leads to an increase of this difference (0.82 ppm), which is again well reproduced by theoretical calculation (0.77 ppm). These δ differences are mostly unchanged upon closing the DTE moiety. Opening the BOX enables the resonance between the iminium function and the DTE, mostly in the inner thiophene ring, which results in the deshielding of H_2 whereas H_1 is almost not impacted. This is supported by the amplitudes and variations of the Mulliken charges of the corresponding CH groups evaluated at the M06/6-311G(d) level. For CH_1, the charge amounts to −0.17/−0.18 e for forms I−II and VII−VIII whereas, for CH_2, the negative charge is reduced to −0.10 e (−0.10 e) for II (VII) in comparison to −0.13 e (−0.16 e) for I (VIII). Then, closing the DTE shifts both protons to higher fields (by 0.6−1.3 ppm according to the calculations and 0.5−0.9 ppm according to experiments) as a result of destroying the aromaticity of both thiophene rings. Whatever the status of the BOX and the DTE, the expected decrease of conjugation along the ethylenic bridge *trans*-to-*cis* isomerization is also well reproduced by the calculation. We can notice its negligible impact on the H_1 chemical shift (less than 0.1 ppm for both calculated and experimental data). On the other hand, in both the experiment and the calculations the *trans*-to-*cis* isomerization induces shielding or deshielding of H_2 by up to 0.6 ppm.

Concerning vinylic ^{1}H, calculated and experimental results both show that H_4 is more shielded than H_3, with differences ranging between 0.7 and 1.8 ppm. Opening the BOX enhances the deshielding of both protons (by as much as 1.5 ppm) whereas closing the DTE ring has a smaller effect; i.e., δ variations are smaller than 0.4 ppm. The *cis*−*trans* isomerization increases the δ values, by 0.2−0.9 ppm, as a function of the state of the BOX and DTE moieties. For the latter, the deshielding is stronger on H_3 provided BOX is open, which is attributed to the acceptor (iminium) π-conjugation effects. Considering the 2-Th-CH═CHMe model compound where $\delta(H_3)$ decreases by 0.26 ppm and $\delta(H_4)$ increases by 0.19 ppm upon *cis* to *trans* conversion enables us to disentangle the effects of *cis*−*trans* isomerization from those of donor/acceptor charge transfer effects and to show that the latter are dominant.

Table 4. B3LYP/6-311+G(2d,p)//M06/6-311G(d) Average ^{1}H NMR Chemical Shifts (ppm) of the 8 States of the BOX−DTE Biphotochrome 1[a]

	state	H_1	H_2	H_3	H_4	H_5	H_6	H_7	H_8
exptl	c-t-o (I)	6.81	7.12	6.92	6.08	[3.38−3.80]	[3.38−3.80]	1.91	1.92
calcd		7.00	7.49	7.07	6.37	[3.42−3.91]	[3.42−3.94]	1.82	1.74
exptl	o-t-o (II)	6.83	7.96	8.39	7.27	4.02	4.65	1.92	2.06
calcd		7.16	8.10	8.73	7.16	4.23	4.45	1.80	2.03
exptl	o-c-o (III)	6.77	7.37	7.47	6.47	3.90	4.43	1.87	1.86
calcd		7.11	7.67	7.84	6.46	4.13	4.46	1.75	1.77
exptl	c-c-o (IV)	6.79	7.21	6.71	5.50	[3.30−3.77]	[3.30−3.77]	1.83	1.83
calcd		7.00	7.58	6.99	5.63	[3.20−3.89]	[3.33−3.93]	1.75	1.80
exptl	c-c-c (V)	6.10	6.40	6.54	5.80	[3.30−3.77]	[3.30−3.77]	2.10	2.03
calcd		6.18	6.29	6.73	6.01	[3.30−3.87]	[3.36−3.83]	2.25	1.96
exptl	o-c-c (VI)	6.20	6.88	7.41	6.71	[3.90−4.60]	[3.90−4.60]	2.12	2.13
calcd		6.38	7.12	7.69	6.68	4.19	4.35	2.16	2.27
exptl	o-t-c (VII)	6.31	7.18	8.22	6.86	4.02	4.60	2.19	2.18
calcd		6.41	7.23	8.39	6.60	4.05	4.36	2.39	2.20
exptl	c-t-c (VIII)	6.16	6.46	6.97	6.04	[3.30−3.80]	[3.30−3.80]	2.08	2.07
calcd		6.26	6.64	6.76	6.01	[3.52−3.90]	[3.42−3.93]	2.24	2.22

[a]In comparison to the experimental values of ref 51 recorded at room temperature (RT), except for VI at 243 K. Solvent effects were taken into account using the IEFPCM scheme (solvent = acetonitrile).

DOI: 10.1021/acs.jpcc.7b11221
J. Phys. Chem. C 2018, 122, 1800−1808

Globally, the calculations reproduce the experimental values as well as the variations upon closing/opening the BOX and DTE units and upon *cis*−*trans* isomerization.

Concerning H_5 and H_6, the closed status of the oxazolidine ring prevents us from assigning their chemical shifts where four different nuclei should be considered. Once BOX opens, one observes that the H_6 protons are more deshielded than the H_5 ones, both experimentally and in the DFT calculations. Moreover, opening/closing the DTE has a small impact on these protons whereas the *cis*−*trans* isomerization presents smaller and less systematic effects.

The calculated and experimental chemical shifts of H_7 and H_8 are systematically smaller when the DTE moiety is open than when closed, due to the loss of thiophene aromaticity in the closed form and due to the change on the hybridization of quaternary carbons upon cyclization ($sp^3 \rightarrow sp^2$). Then, the difference between $\delta(H_7)$ and $\delta(H_8)$ is generally very small (for either calculations or experiments; forms I, III, IV, VI, VIII), on the order of 0.1 ppm or smaller, demonstrating a similar chemical environment for these methyl protons.

For the three couples H_1−H_2, H_3−H_4, and H_7−H_8, least-squared linear regressions have been performed to quantify the agreement between the experimental and calculated chemical shifts (Figure 2), showing r^2 values of 0.95 or slightly larger for H_1−H_4 and of 0.89 for H_7 and H_8. As mentioned above, the signal complexity and impossible assignment of H_5 and H_6 protons when BOX is closed render similar regression for this couple irrelevant. For H_1−H_4 the slopes of the linear regressions are smaller than 1.0 (by 14% and 9% for H_1−H_2 and H_3−H_4, respectively), demonstrating that calculated δ variations are slightly overestimated with respect to experiment. On the other hand, the slope is clearly smaller than unity for H_7−H_8.

III.C. Conformational Effects on the NMR Signatures of the c-t-o (I) and o-t-o (II) States of Compounds 1 and 2. Having assessed the reliability of the ^{1}H NMR chemical shift calculations, the question is now to investigate whether the presence of folded conformers in state I versus state II would be visible in the NMR signatures; i.e., whether the two categories of conformers have distinct chemical shifts. Since the experimental structural characterizations are based on the Me ^{1}H, the chemical shifts of H_7 and H_8 were evaluated for the eight conformers of compounds **1** and **2** in states I and II. They can be found in Table 5 with their weighted averages as a function of the relative electronic energies, enthalpies, and Gibbs free energies (highlighting thermal and entropic effects) as well as the experimental values.[24,51]

Concerning the methyl protons of both compounds under state I, the antiparallel (parallel) conformers are characterized by H_7 having a chemical shift smaller (higher) than 2.0 ppm and by H_8 being always below the same 2.0 ppm limit, with the exception of conformer h of **2** for which the H_7 and H_8 behaviors are reversed. Under state **I**, the most deshielded shifts are observed for H_7 in the parallel conformers at around 2.4 and 2.7 ppm for compounds **1** and **2**, respectively. Then, considering compound **1** under state II, the same H_7 behavior is observed, but the H_8 protons are overall more deshielded than in state I, especially in the case of the parallel conformers where their chemical shifts now exceed 2.1 ppm. Finally, for state II of compounds **1** and **2**, there is no systematic behavior among H_7 or H_8, but the antiparallel conformers are characterized by one of its protons being around 1.9 ppm and the second one around 2.0 ppm while in the parallel conformers they are less shielded (about 2 and 2.8 ppm). In general, folding the thiophene rings on each other deshields the methyl protons as a result of the anisotropic effect.

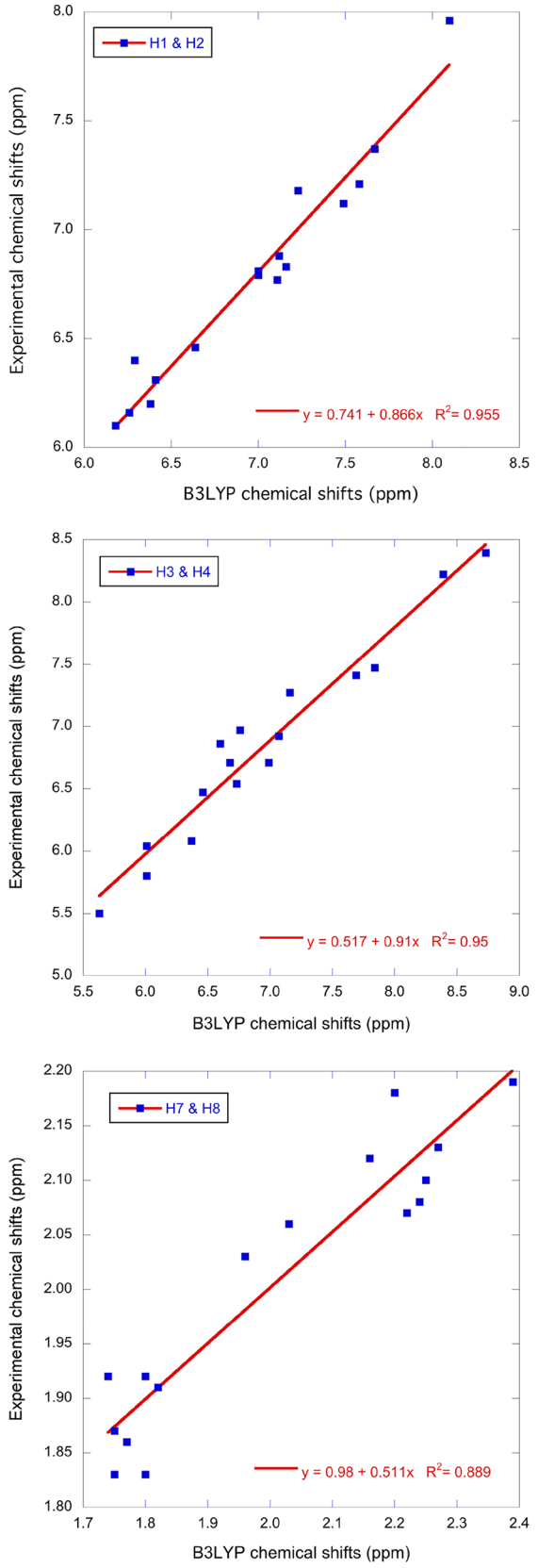

Figure 2. Experimental versus B3LYP ^{1}H chemical shifts for the H_1−H_4 and H_7−H_8 protons of the 8 states of the BOX−DTE **1** switch.

DOI: 10.1021/acs.jpcc.7b11221
J. Phys. Chem. C 2018, 122, 1800−1808

Table 5. B3LYP/6-311+G(2d,p)//M06/6-311G(d) ^{1}H NMR Chemical Shifts (ppm) of Compounds 1 and 2 in Their c-t-o (I) and o-t-o (II) States[a]

	c-t-o (I)		o-t-o (II)	
conformer	H_7	H_8	H_7	H_8
	Compound **1**			
a	1.85	1.77	1.79	2.03
b	1.81	1.76	1.85	1.91
c	1.81	1.78	1.84	1.98
d	1.85	1.76	1.84	1.86
e	2.37	1.86	2.61	2.88
f	2.39	1.74	2.27	2.17
g	2.41	1.78	2.56	2.86
h	2.36	1.90	2.29	2.13
av (ΔE_{elec})	1.86	1.77	1.85	2.01
av ($\Delta H°$)	1.86	1.77	1.85	2.01
av ($\Delta G°$)	1.89	1.77	1.87	2.01
exptl	1.91	1.92	1.92	2.06
	Compound **2**			
a	1.84	1.80	1.87	2.05
b	1.87	1.81	1.89	2.01
c	1.86	1.81	1.86	1.98
d	1.88	1.83	2.00	1.92
e	2.73	1.87	1.96	2.97
f	2.71	1.88	2.72	2.11
g	2.76	1.96	1.86	2.86
h	1.94	2.74	2.71	2.04
av (ΔE_{elec})	2.03	1.84	1.89	2.27
av ($\Delta H°$)	2.00	1.83	1.89	2.25
av ($\Delta G°$)	1.88	1.84	1.88	2.07
exptl	2.03	1.99	2.04	2.13

[a]In addition to the values for the eight most stable conformers, Maxwell−Boltzmann averages are given using the total electronic energy, the enthalpy, and the Gibbs enthalpy differences as well as the experimental values of refs 51 and 24. Conformers a−d (e−h) are unfolded (folded). Solvent effects were taken into account using the IEFPCM scheme (solvent = acetonitrile).

For compound **1**, the averages calculated for both states show almost no variation among each other, i.e., whether they are calculated from the electronic energies, enthalpies, or Gibbs free energies. Thus, going from state I to state II, the chemical shift of H_7 is hardly changed whereas it increases by 0.24 ppm for H_8. These averages are also in good agreement with the previously discussed results obtained for the antiparallel conformers (Section III.A, Table 4). For compound **2**, the averages based on the electronic energy and the enthalpy are consistent, showing a significant decrease (with respect to compound **1**) of the shielding for H_7 in state I (0.15 ppm) and for H_8 in state II (0.25 ppm) due to a larger contribution of the parallel conformers (see Section III.A, Table 3). As a matter of fact, H_7 gets more shielded (~0.11 ppm), and H_8 gets more deshielded (~0.42 ppm) when going from state I to state II. The averages based on the Gibbs free energy do not show this behavior (or it is reduced in amplitude), most probably because the entropic effects are overestimated.

IV. CONCLUSIONS

Density functional theory has been used to investigate the relationships between the structures, energies, and NMR signatures of an octastate molecular switch, that is composed of a dithienylethene (DTE) unit covalently linked to an indolino[2,1-*b*]oxazolidine (BOX) moiety through an ethylenic junction. Both the DTE and BOX moieties can adopt open or closed forms while the ethylenic junction can be *Z* or *E*. In the first part, the *E* conformer has been confirmed to be, by far, more stable than the *Z* one for all BOX/DTE combinations. Then, when the DTE is open, the two thienyl units can fold to form parallel conformers, by opposition to the antiparallel or unfolded conformers. Parallel conformers present a higher energy than the antiparallel ones. Still, in the case of compound **2** having a bulky substituent (R = *p*Ph-SMe) on the terminal thienyl group, the enthalpy of one conformer is very close (1−2 kJ mol^{-1}) to that of the most stable antiparallel one, making photocyclization less efficient. Less favorable intermolecular interactions are present in compound **1** (R = Me) as compared to those in compound **2** so that the enthalpy of the parallel conformers of **1** is higher by 6−7 kJ mol^{-1} than that of the antiparallel ones. In a second part, ^{1}H NMR chemical shifts calculations have been carried out on the different parallel and antiparallel conformers of compounds **1** and **2** when DTE is open to highlight the presence of parallel DTE forms. The reliability of these calculations was substantiated by a preliminary comparison between the calculated and experimental ^{1}H NMR chemical shifts of the 8 states of compound **1** providing least-squares linear regressions with r^2 values larger than ~0.90. The analysis of the calculated ^{1}H NMR chemical shifts shows that, in agreement with the experimental data, (i) going from state I to state II, the H_8 proton of compound **1** is deshielded by ~0.15 ppm, (ii) the deshielding of H_8 proton of compound **2** is larger and attains 0.41 ppm whereas H_7 is more shielded by 0.11 ppm, and (iii) then, going from compound **1** to compound **2** leads to deshielding of both H_7 and H_8 protons. As a consequence, we can now assume that the difference of photochromism gating efficiency among compounds **1**, **2**, and **3** results mainly from the stabilization of the parallel conformer due to an establishment of an intramolecular interaction with BOX opening in addition to the previously mentioned electronic effect.

AUTHOR INFORMATION

Corresponding Authors

*E-mail: benoit.champagne@unamur.be.
*E-mail: lionel.sanguinet@univ-angers.fr.

ORCID

Lionel Sanguinet: 0000-0002-4334-9937
Benoît Champagne: 0000-0003-3678-8875

Author Contributions

⊥S.H.M. and J.Q. contributed equally.

Notes

The authors declare no competing financial interest.

ACKNOWLEDGMENTS

This work, carried out within the MORIARTY project, has benefited from financial support from Wallonie-Bruxelles International (WBI), from the Fund for Scientific Research (F.R.S.-FNRS), from the French Ministry of Foreign and European Affairs, and from the Ministry of Higher Education and Research in the frame of the Hubert Curien partnerships. S.H.M. thanks the Fonds Spécial de Recherche of UNamur for his Ph.D. grant while J.Q. thanks the "Actions de Recherche Concertées" (ARC) of the Direction générale de l'Enseignement non Obligatoire et de la Recherche Scientifique of the French Community of Belgium, under convention no. 15/20-

DOI: 10.1021/acs.jpcc.7b11221
J. Phys. Chem. C 2018, 122, 1800−1808

068, for his Ph.D. grant. This work was also supported by funds from the Francqui Foundation. S.D. and L.S. thank ANR SIMI 7 for financial support (grant no.: 2011 BS08 007 02). The calculations were performed on the computers of the Consortium des Équipements de Calcul Intensif, including those of the Technological Platform of High-Performance Computing, for which we gratefully acknowledge the financial support of the FNRS-FRFC (Conventions No. 2.4.617.07.F and 2.5020.11) and of the University of Namur.

REFERENCES

(1) Andréasson, J.; Pischel, U. Smart Molecules at Work-Mimicking Advanced Logic Operations. *Chem. Soc. Rev.* **2010**, *39*, 174−188.
(2) Andréasson, J.; Pischel, U. Molecules with a Sense of Logic: a Progress Report. *Chem. Soc. Rev.* **2015**, *44*, 1053−1069.
(3) Irie, M.; Fukaminato, T.; Matsuda, K.; Kobatake, S. Photochromism of Diarylethene Molecules and Crystals: Memories, Switches, and Actuators. *Chem. Rev.* **2014**, *114*, 12174−12277.
(4) de Silva, A. P.; Vance, T. P.; Wannalerse, B.; West, M. E. S. Molecular Logic Systems. In *Molecular Switches*; Wiley-VCH: Weinheim, 2011; pp 669−696.
(5) Minkin, V. I. Photoswitchable Molecular Systems Based on Spiropyrans and Spirooxazines. In *Molecular Switches*; Wiley-VCH: Weinheim, 2011; pp 37−80.
(6) *Molecular Switches*, 2nd ed.; Feringa, B. L., Browne, W. R., Eds.; Wiley-VCH: Weinheim, 2011.
(7) Oms, O.; Hakouk, K.; Dessapt, R.; Deniard, P.; Jobic, S.; Dolbecq, A.; Palacin, T.; Nadjo, L.; Keita, B.; Marrot, J.; Mialane, P. Photo- and Electrochromic Properties of Covalently Connected Symmetrical and Unsymmetrical Spiropyran−Polyoxometalate Dyads. *Chem. Commun.* **2012**, *48*, 12103−12105.
(8) Browne, W. R.; Pollard, M. M.; de lange, B.; Meetsma, A.; Feringa, B. L. Reversible Three-State Switching of Luminescence: A New Twist to Electro- and Photochromic Behavior. *J. Am. Chem. Soc.* **2006**, *128*, 12412−12413.
(9) Ivashenko, O.; Logtenberg, H.; Areephong, J.; Coleman, A. C.; Wesenhagen, P. V.; Geertsema, E. M.; Heureux, N.; Feringa, B. L.; Rudolf, P.; Browne, W. R. Remarkable Stability of High Energy Conformers in Self-Assembled Monolayers of a Bistable Electro- and Photoswitchable Overcrowded Alkene. *J. Phys. Chem. C* **2011**, *115*, 22965−22975.
(10) Harvey, E. C.; Feringa, B. L.; Vos, J. G.; Browne, W. R.; Pryce, M. T. Transition Metal Functionalized Photo- and Redox-Switchable Diarylethene Based Molecular Switches. *Coord. Chem. Rev.* **2015**, *282*, 77−86.
(11) Bondu, F.; Quertinmont, J.; Rodriguez, V.; Pozzo, J.-L.; Plaquet, A.; Champagne, B.; Castet, F. Second-Order Nonlinear Optical Properties of a Dithienylethene-Indolinooxazolidine Hybrid: A Joint Experimental and Theoretical Investigation. *Chem. - Eur. J.* **2015**, *21*, 18749−18757.
(12) Szalóki, G.; Pozzo, J.-L. Synthesis of Symmetrical and Nonsymmetrical Bisthienylcyclopentenes. *Chem. - Eur. J.* **2013**, *19*, 11124−11132.
(13) Fukaminato, T. Single-molecule fluorescence photoswitching: Design and Synthesis of Photoswitchable Fluorescent Molecules. *J. Photochem. Photobiol., C* **2011**, *12*, 177−208.
(14) Bertarelli, C.; Bianco, A.; Castagna, R.; Pariani, G. Photochromism into Optics: Opportunities to Develop Light-Triggered Optical Elements. *J. Photochem. Photobiol., C* **2011**, *12*, 106−125.
(15) Tsujioka, T.; Irie, M. Electrical Functions of Photochromic Molecules. *J. Photochem. Photobiol., C* **2010**, *11*, 1−14.
(16) Irie, M. Photochromism of Diarylethene Single Molecules and Single crystals. *Photoch. Photobio. Sci.* **2010**, *9*, 1535−1542.
(17) Yun, C.; You, J.; Kim, J.; Huh, J.; Kim, E. Photochromic Fluorescence Switching from Diarylethenes and its Applications. *J. Photochem. Photobiol., C* **2009**, *10*, 111−129.
(18) Wigglesworth, T. J.; Myles, A. J.; Branda, N. R. High-Content Photochromic Polymers Based on Dithienylethenes. *Eur. J. Org. Chem.* **2005**, *2005*, 1233−1238.
(19) Tian, H.; Yang, S. J. Recent Progresses on Diarylethene Based Photochromic Switches. *Chem. Soc. Rev.* **2004**, *33*, 85−97.
(20) Matsuda, K.; Irie, M. Diarylethene as a Photoswitching Unit. *J. Photochem. Photobiol., C* **2004**, *5*, 169−182.
(21) Gust, D.; Andréasson, J.; Pischel, U.; Moore, T. A.; Moore, A. L. Data and Signal Processing Using Photochromic Molecules. *Chem. Commun.* **2012**, *48*, 1947−1957.
(22) Irie, M. Diarylethenes for Memories and Switches. *Chem. Rev.* **2000**, *100*, 1685−1716.
(23) Tomasulo, M.; Sortino, S.; Raymo, F. M. A Fast and Stable Photochromic Switch Based on the Opening and Closing of an Oxazine Ring. *Org. Lett.* **2005**, *7*, 1109−1112.
(24) Sanguinet, L.; Delbaere, S.; Berthet, L.; Szalóki, G.; Jardel, D.; Pozzo, J.-L. Dithienylethene-Based Gated Ambichromic Dyads. *Adv. Opt. Mater.* **2016**, *4*, 1358−1362.
(25) Jacquemin, D.; Perpète, E. A.; Maurel, F.; Perrier, A. Photochromic Properties of a Dithienylethene-Indolinooxazolidine Switch: A Theoretical Investigation. *Comput. Theor. Chem.* **2011**, *963*, 63−70.
(26) Nakamura, S.; Yokojima, S.; Uchida, K.; Tsujioka, T.; Goldberg, A.; Murakami, A.; Shinoda, K.; Mikami, M.; Kobayashi, T.; Kobatake, S.; Matsuda, K.; Irie, M. Theoretical Investigation on Photochromic Diarylethene: A Short Review. *J. Photochem. Photobiol., A* **2008**, *200*, 10−18.
(27) Helgaker, T.; Jaszunski, M.; Ruud, K. *Ab Initio* Methods for the Calculation of NMR Shielding and Indirect Spin-Spin Coupling Constants. *Chem. Rev.* **1999**, *99*, 293−472.
(28) *Calculation of NMR and EPR Parameters*; Kaupp, M., Bühl, M., Malkin, V. G., Eds.; Wiley-VCH: Weinheim, 2004.
(29) Bifulco, G.; Dambruoso, P.; Gomez-Paloma, L.; Riccio, R. Determination of Relative Configuration in Organic Compounds by NMR Spectroscopy and Computational Methods. *Chem. Rev.* **2007**, *107*, 3744−3779.
(30) Ochsenfeld, C.; Kussmann, J.; Koziol, F. Ab Initio NMR Spectra for Molecular Systems with a Thousand and More Atoms: A Linear-Scaling Method. *Angew. Chem., Int. Ed.* **2004**, *43*, 4485−4489.
(31) Chesnut, D. B. *The Ab Initio Computation of Nuclear Magnetic Resonance Chemical Shielding*; Wiley-VCH: Weinheim, 1996; Vol. *8*.
(32) Rablen, P. R.; Pearlman, S. A.; Finkbiner, J. A Comparison of Density Functional Methods for the Estimation of Proton Chemical Shifts with Chemical Accuracy. *J. Phys. Chem. A* **1999**, *103*, 7357−7363.
(33) d'Antuono, P.; Botek, B.; Champagne, B.; Spassova, M.; Denkova, P. Theoretical Investigation on ^{1}H and ^{13}C NMR Chemical Shifts of Small Alkanes and Chloroalkanes. *J. Chem. Phys.* **2006**, *125*, 144309.
(34) Laskowski, R.; Blaha, P.; Tran, F. Assessment of DFT Functionals with NMR Chemical Shifts. *Phys. Rev. B: Condens. Matter Mater. Phys.* **2013**, *87*, 195130.
(35) Flaig, D.; Maurer, M.; Hanni, M.; Braunger, K.; Kick, L.; Thubauville, M.; Ochsenfeld, C. Benchmarking Hydrogen and Carbon NMR Chemical Shifts at HF, DFT, and MP2, Levels. *J. Chem. Theory Comput.* **2014**, *10*, 572−578.
(36) Toomsalu, E.; Burk, P. Critical Test of Some Computational Methods for Prediction of NMR ^{1}H and ^{13}C Chemical Shifts. *J. Mol. Model.* **2015**, *21*, 244.
(37) Mugridge, J. S.; Bergman, R. G.; Raymond, K. N. ^{1}H NMR Chemical Shift Calculations as a Probe of Supramolecular Host-Guest Geometry. *J. Am. Chem. Soc.* **2011**, *133*, 11205−11212.
(38) Dyson, B. S.; Burton, J. W.; Sohn, T.; Kim, B.; Bae, H.; Kim, D. Total Synthesis and Structure Confirmation of Elatenyne: Success of Computational Methods for NMR Prediction with Highly Flexible Diastereomers. *J. Am. Chem. Soc.* **2012**, *134*, 11781−11790.
(39) Kutateladze, A. G.; Mukhina, O. A. Relativistic Force Field: Parametric Computations of Proton-Proton Coupling Constants in ^{1}H NMR Spectra. *J. Org. Chem.* **2014**, *79*, 8397−8406.

DOI: 10.1021/acs.jpcc.7b11221
J. Phys. Chem. C 2018, 122, 1800−1808

(40) Hricovini, M.; Driguez, P.; Malkina, O. L. NMR and DFT Analysis of Trisaccharide from Heparin Repeating Sequence. *J. Phys. Chem. B* **2014**, *118*, 11931−11942.
(41) Trabelsi, M.; Salem, M.; Champagne, B. Investigation of the Configuration of Alkyl Phenyl Ketone Phenylhydrazones from *Ab Initio* ^{1}H NMR Chemical shifts. *Org. Biomol. Chem.* **2003**, *1*, 3839−3844.
(42) d'Antuono, P.; Botek, E.; Champagne, B.; Wieme, J.; Reyniers, M. F.; Marin, G. B.; Adriaensens, P. J.; Gelan, J. A Joined Theoretical-Experimental Investigation on the ^{1}H and ^{13}C NMR Signatures of Defects in Poly(vinyl chloride). *J. Phys. Chem. B* **2008**, *112*, 14804−14818.
(43) Smith, S. G.; Goodman, J. M. Assigning the Stereochemistry of Pairs of Diastereoisomers Using GIAO NMR Shift Calculation. *J. Org. Chem.* **2009**, *74*, 4597−4607.
(44) Kleinpeter, E.; Lämmermann, A.; Kühn, H. Synthesis and NMR Spectra of the Syn and Anti Isomers of Substituted Cyclobutanes-Evidence for Steric and Spatial Hyperconjugative Interactions. *Tetrahedron* **2011**, *67*, 2596−2604.
(45) Bartlett, M. J.; Northcote, P. T.; Lein, M.; Harvey, J. E. ^{13}C NMR Analysis of 3,6-Dihydro-2H-pyrans: Assignment of Remote Stereochemistry Using Axial Shielding Effects. *J. Org. Chem.* **2014**, *79*, 5521−5532.
(46) Zhao, Y.; Truhlar, D. G. The M06 Suit of Density Functionals for Main Group Thermochemistry, Thermochemical Kinetics, Noncovalent Interactions, Excited States, and Transition Element: Two New Functionals and Systematic Testing of Four M06-Class Functionals and 12 Other Functionals. *Theor. Chem. Acc.* **2008**, *120*, 215−241.
(47) Cheeseman, J. R.; Trucks, G. W.; Keith, T. A.; Frisch, M. J. A Comparison of Models for Calculating Nuclear Magnetic Resonance Shielding Tensors. *J. Chem. Phys.* **1996**, *104*, 5497−5509.
(48) Diliën, H.; Marin, L.; Botek, E.; Champagne, B.; Lemaur, V.; Beljonne, D.; Lazzaroni, R.; Cleij, T. J.; Maes, W.; Lutsen, L.; Vanderzande, D.; Adriaensens, P. J. Fingerprints for Structural Defects in Poly(thienylene vinylene) (PTV): A Joint Theoretical-Experimental NMR Study on Model Molecules. *J. Phys. Chem. B* **2011**, *115*, 12040−12050.
(49) Tomasi, J.; Mennucci, B.; Cammi, R. Quantum Mechanical Continuum Solvation Models. *Chem. Rev.* **2005**, *105*, 2999−3093.
(50) Frisch, M. J.; Trucks, G W.; Schlegel, H. B.; Scuseria, G. E.; Robb, M. A.; Cheeseman, J. R.; Scalmani, G.; Barone, V.; Mennucci, B.; Petersson, G. A.; et al. *Gaussian 09, revision A.01*; Gaussian, Inc.: Wallingford, CT, 2010.
(51) Szalóki, G.; Sevez, G.; Berthet, J.; Pozzo, J.-L.; Delbaere, S. A Simple Molecule-Based Octastate Switch. *J. Am. Chem. Soc.* **2014**, *136*, 13510−13513.

DOI: 10.1021/acs.jpcc.7b11221
J. Phys. Chem. C 2018, 122, 1800−1808